



Universidad
de Oviedo

C. Bayón-Cueli

Polytechnic School of Engineering of Gijón, University of Oviedo, Spain

A. Barbón

Department of Electrical Engineering, University of Oviedo, Campus of Gijón, Spain

L. Bayón

Department of Mathematics, University of Oviedo, Campus of Gijón, Spain,

A. Fernández-Conde

Polytechnic School of Engineering of Gijón, University of Oviedo, Spain

Introduction

The continual lowering of costs for photovoltaic (PV) systems components has led to an unprecedented growth in solar energy generation. The weighted average of the levelized cost of energy (LCOE) in 2018 was 0.085 (USD/kWh), and it's forecasted to be between 0.02 and 0.08 (USD/kWh) by 2030, and between 0.014 and 0.05 (USD/kWh) by 2050 [1]. The design of the PV plants, is directly related to such costs although many different variables are to be considered [2]. The racking systems and the characteristics of the land are two fundamental variables. Land cost can be estimated of more than 5% of total project budget.

The racking systems for the modules used in PV systems can be classified into two types: those with a fixed tilt angle and those with variable tilt angle (dual-axis trackers, single-axis trackers).

The single-axis trackers can have different orientations: horizontal North-South, horizontal East-West, and parallel to the Earth's axis. In practice, North-South aligned systems are the most commonly used, though for higher accuracy, more expensive dual-axis trackers can be implemented.

The availability of flat land is related to the decrease in the cost of PV plants. However, there are areas where flat land is not available and the terrain slope largely influences the electrical output and construction costs of large-scale PV plants [3].

A common criterion on the maximum terrain slope accepted in this type of installations has not yet been reached. For example, Yushchenko et al. [4] proposes the criterion of 5.71° (or 10%) of terrain slope, Alami et al. [5] accepted a maximum of 5% terrain slope and IRENA [6] proposes the criterion of 11.3° (or 20%). The single-axis tracker aligned with the North-South axis were designed for the installation on flat terrain. Considering that this tracker is the most common solution for installing large solar projects, it is necessary to conduct a study of their performance in installations on sloping terrain. This paper deals with the relationship between terrain slope and energy yield of a single-axis tracker aligned with the North-South axis. Said tracking geometry has been reviewed developing operating equations and carrying out simulations for different locations and slopes of terrain.

Solar tracking geometry

Fig.1 shows the solar geometry used in the current study.

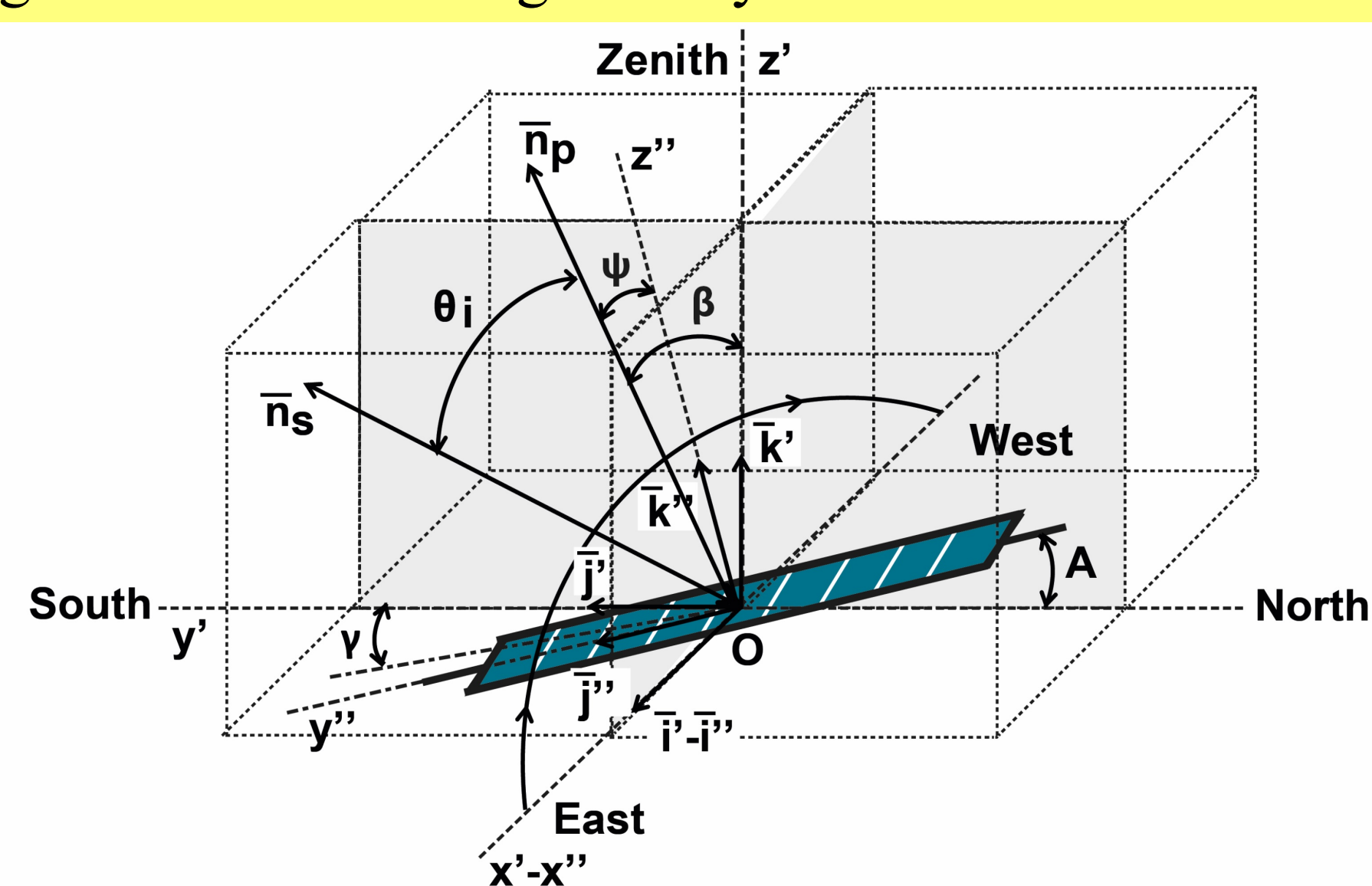


Fig. 1. Solar geometry used in the current study.

The solar position can be determined by a unit vector always orientated to said star, called solar vector \bar{n}_s , which can be represented by eq. (global reference system):

$$\bar{n}_s = (\sin\omega \cos\delta, \cos\omega \cos\delta, \sin\delta) \cdot (\bar{i}, \bar{j}, \bar{k})$$

where: δ - solar declination, rad; ω - hour angle, rad. If the Earth reference system is used, the solar vector can be represented by eq.:

$$\bar{n}_s = (\sin\omega \cos\delta, \cos\omega \cos\delta, \sin\delta) \cdot \begin{pmatrix} 1 & 0 & 0 \\ 0 & \sin\lambda & \cos\lambda \\ 0 & -\cos\lambda & \sin\lambda \end{pmatrix} \cdot \begin{pmatrix} \bar{i}'' \\ \bar{j}'' \\ \bar{k}'' \end{pmatrix}$$

where: λ - latitude, rad. Taking into account the terrain slope results in some changes to these equations. For this purpose, the axis of the solar tracker is considered to form an angle A with the horizontal. In this reference system, the solar vector can be represented by eq.:

$$\bar{n}_s = (\sin\omega \cos\delta, \cos\omega \cos\delta \sin\lambda - \sin\delta \cos\lambda, \cos\omega \cos\delta \cos\lambda + \sin\delta \sin\lambda) \cdot \begin{pmatrix} 1 & 0 & 0 \\ 0 & \cos A & \sin A \\ 0 & -\sin A & \cos A \end{pmatrix} \cdot \begin{pmatrix} \bar{i}'' \\ \bar{j}'' \\ \bar{k}'' \end{pmatrix}$$

The vector normal to the collector surface, \bar{n}_p , can be deduced:

$$\bar{n}_p = (\sin\psi, 0, \cos\psi) \cdot (\bar{i}'', \bar{j}'', \bar{k}'')$$

where: ψ - angle between \bar{n}_p and Oz'' , rad. This angle can be calculated using the tracking condition:

$$\tan\psi = \frac{\sin\omega \cos\delta}{\cos\omega \cos\delta \cos(\lambda - A) + \sin\delta \sin(\lambda - A)}$$

The incident angle can be calculated:

$$\cos\theta = \frac{\bar{n}_s \cdot \bar{n}_p}{|\bar{n}_s| \cdot |\bar{n}_p|}$$

After complex operations to eliminate ψ , the incident angle can be calculated:

$$\cos\theta = \cos\delta \sqrt{\frac{\sin^2\omega + (\cos\omega \cos(\lambda - A) + \tan\delta \sin(\lambda - A))^2}{\cos^2\omega \cos^2\delta + \sin^2\delta}}$$

The tilt angle can be calculated:

$$\cos\beta = \bar{n}_p \cdot \bar{k}'$$

Performing mathematical operations, the tilt angle is:

$$\beta = \arccos \left(\frac{\cos A (\cos\omega \cos\delta \cos(\lambda - A) + \sin\delta \sin(\lambda - A))}{\cos\theta} \right)$$

Results and discussions

In this study several cities around the World are considered. Tab.1 shows the geographic characteristics of said cities.

Table 1. Cities under study.

Cities	Latitude	Longitude	Altitude
Medellin (Colombia).	06°14'38"N	75°34'04"W	1469 (m)
Bangkok (Thailand).	13°45'14"N	100°29'34"E	9 (m)
Morelia (Mexico).	19°42'10"N	101°11'24"W	1921 (m)
Karachi (Pakistan).	24°52'01"N	67°01'51"E	14 (m)
Cairo (Egypt).	30°29'24"N	31°14'38"W	41 (m)
Almeria (Spain).	36°50'07"N	02°24'08"W	22 (m)
Toronto (Canada).	43°39'14"N	79°23'13"W	106 (m)
Wien (Austria).	48°15'00"N	16°21'00"E	203 (m)
Hamburg (Germany).	53°33'00"N	10°00'03"E	19 (m)
Helsinki (Finland).	60°10'10"N	24°56'07"E	23 (m)

Influence of the terrain slope on $\cos\theta$

Fig. 2 shows the $\cos\theta$ depending on the time of day and the day of year, in Medellin and Helsinki, respectively.

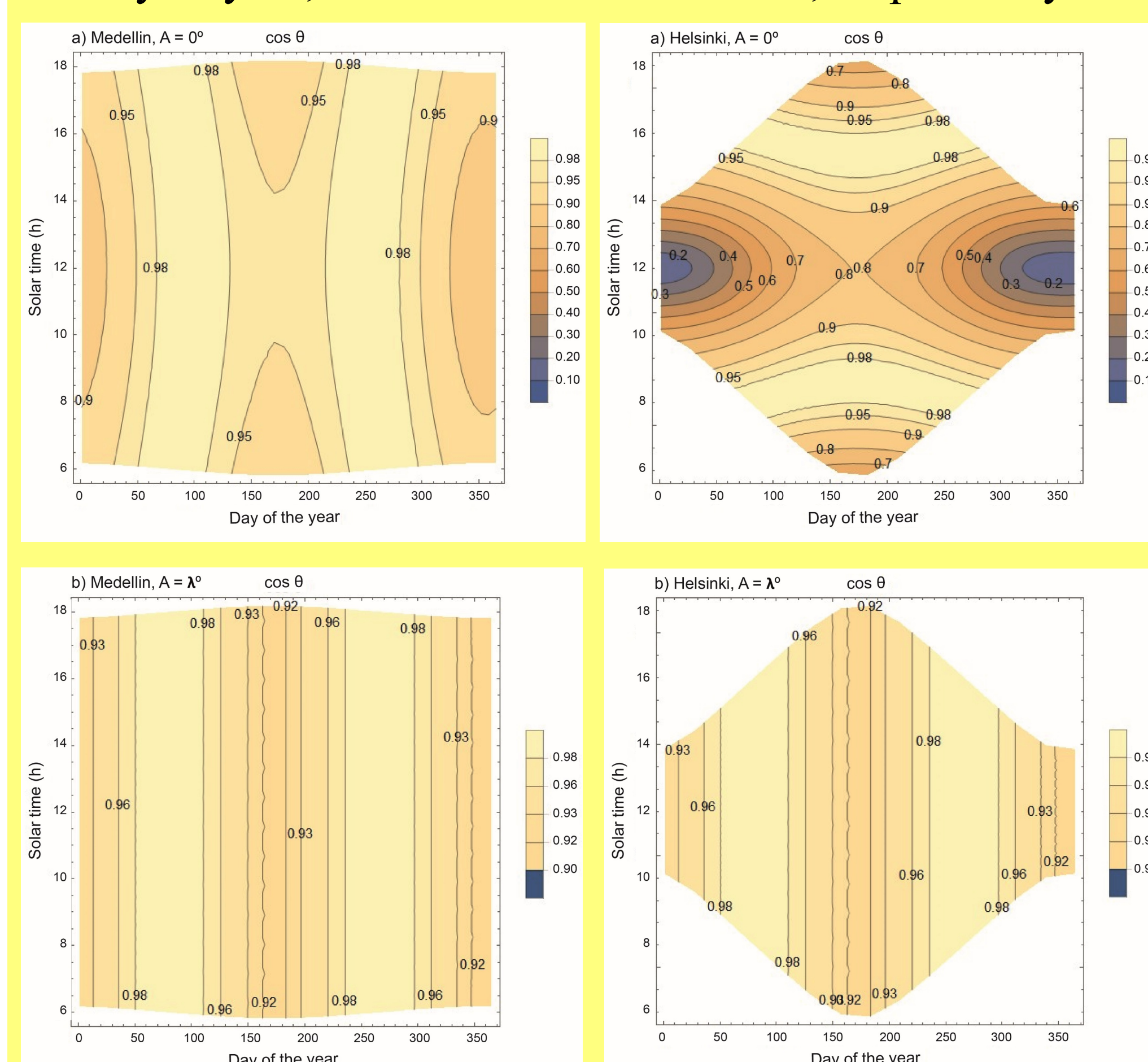


Fig. 2. $\cos\theta$ for the cities of Medellin and Helsinki.

For $A=0$ (°) is noted that in the lowest latitude location (Medellin) a better $\cos\theta$ is gotten compared to the rest of the locations, especially in the winter months. As the latitude of the location increases, the $\cos\theta$ decreases. Therefore, the astronomical tracking systems yield better results in lower latitude locations.

For $A=\lambda$ (°) is noted that similar values of $\cos\theta$ are obtained in all two locations.

Influence of the terrain slope on annual energy

Fig. 3 shows of annual energy in the cities under study. The values are as a percentage of energy, with respect to the $A=0$ (°) situation, that is:

$$E = \frac{H_t^\lambda - H_t^0}{H_t^0} * 100$$

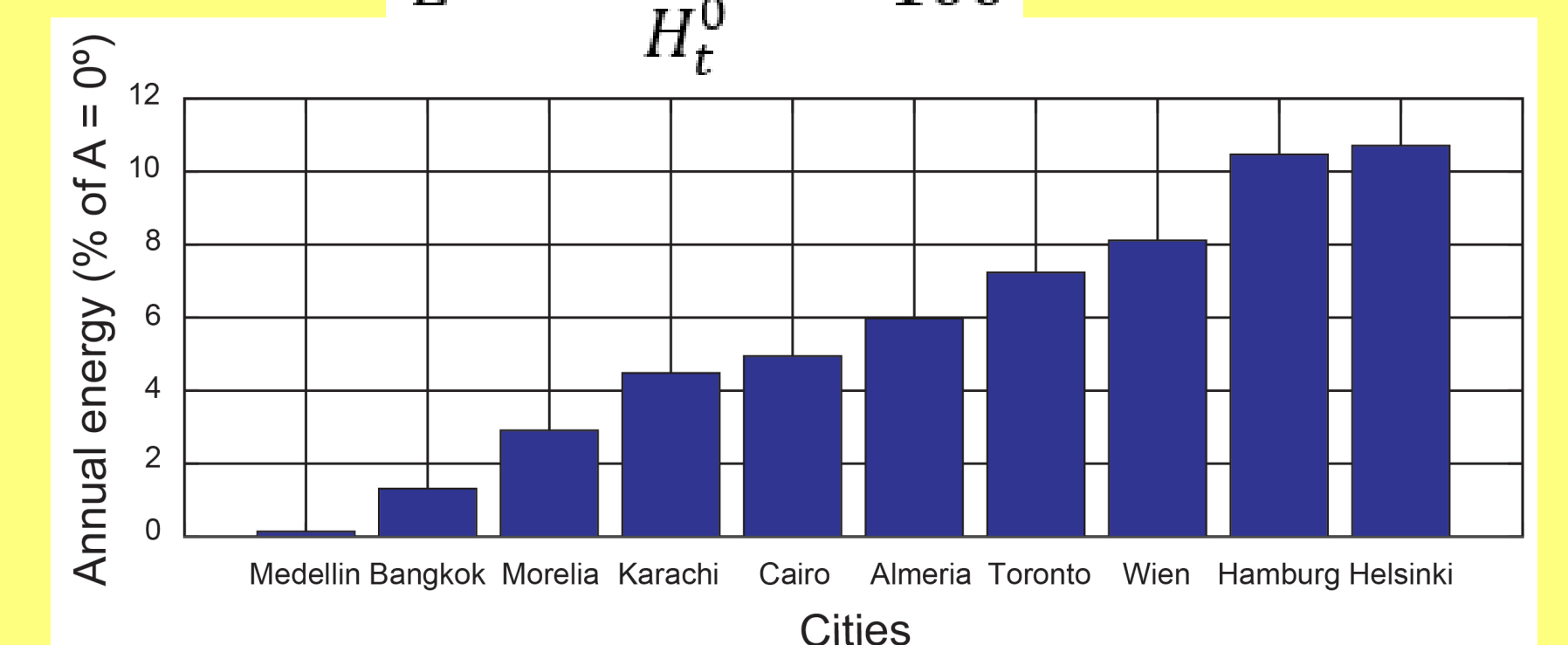


Fig. 3. Comparison annual energy.

An increase in terrain slope increases the energy generated, an effect which is most pronounced as latitude increases. The percentage of the energy gains associated with terrain slope, referenced to flat terrain ranges from 0.14% (low latitude) to 10.71% (high latitude).

Conclusions

The main conclusions drawn from all these work are:

- In all climate areas the terrain slope increases both the annual energy and the $\cos\theta$.
- For flat terrains the value of $\cos\theta$ is considerably greater as latitude decreases, so it can be concluded that astronomical tracking yields better results in lower latitude locations.
- As the slope of the terrain increases such difference between latitudes is diminished, with annual energy production increasing for all locations, more remarkably in those locations of higher latitude.
- The percentage of the energy gains associated with terrain slope, referenced to flat terrain, ranges from a merely 0.1 – 0.2% in low latitudes to over 10% for PV systems at high latitudes.

References

- [1] IRENA. Future of solar photovoltaic: Deployment, investment, technology, grid integration and socio-economic aspects; 2019. International Renewable Energy Agency, <https://www.irena.org/>
- [2] S.K. Saraswat, A.K. Digalwar, S.S. Yadav, G. Kumar. MCDM and GIS based modelling technique for assessment of solar and wind farm locations in India. *Renewable Energy* **169**, 865-884 (2021).
- [3] J.R.S. Doorga, S.D.D.V. Rughoputh, R. Boojhawon. Multi-criteria GIS-based modelling technique for identifying potential solar farm sites: A case study in Mauritius. *Renewable Energy* **133**, 1201-1219 (2019).
- [4] A. Yushchenko, A. Bono, B. Chatenoux, M.K. Patel, N. Ray. GIS-based assessment of photovoltaic (PV) and concentrated solar power (CSP) generation potential in West Africa. *Renewable and Sustainable Energy Reviews* **81**, 2088-2103 (2018).
- [5] A. Alami Merrouni, F. Elwali Elalaoui, A. Mezhrab, A. Mezhrab, A. Ghennioui. Large scale PV sites selection by combining GIS and Analytical Hierarchy Process. Case study: Eastern Morocco. *Renewable Energy* **119**, 863-873 (2018).
- [6] IRENA. Unleashing the solar potential in ECOWAS: Seeking areas of opportunity for grid-connected and decentralised PV applications. International Renewable Energy Agency, 2013.
- [7] J.A. Duffie, W.A. Beckman. *Solar Engineering of Thermal Processes*. John Wiley & Sons, 2013.
- [8] T.O. Kaddoura, M.A.M. Ramli, Y.A. Al-Turki. On the estimation of the optimum tilt angle of PV panel in Saudi Arabia. *Renewable and Sustainable Energy Reviews* **65**, 626-634 (2016).
- [9] K.N. Shukla, S. Rangnekar, K. Sudhakar. Comparative study of isotropic and anisotropic sky models to estimate solar radiation incident on tilted surface: A case study for Bhopal, India. *Energy Reports* **1**, 96-103 (2015).
- [10] E.D. Mehleri, P.L. Zervas, H. Sarimveis, J.A. Palyvos, N.C. Markatos. Determination of the optimal tilt angle and orientation for solar photovoltaic arrays. *Renewable Energy* **35**, 2468-2475 (2010).
- [11] B.Y.H. Liu, R.C. Jordan. The long-term average performance of flat-plate solar energy collectors. *Solar Energy* **7**, 53-74 (1963).
- [12] ASHRAE. *Handbook: HVAC applications*. Chapter 32. Atlanta (GA), ASHRAE, 1999.
- [13] C. Vernay, S. Pitaval, P. Blanc. Review of satellite-based surface solar irradiation databases for the engineering, the financing and the operating of photovoltaic systems. *Energy Procedia* **57**, 1383-1391 (2014).
- [14] M. Paulescu, L. Fara, E. Tulcan-Paulescu. Models for obtaining daily global solar irradiation from air temperature data. *Atmospheric Research* **79**, 227-240 (2006).
- [15] A. Barbón, P. Fortuny Ayuso, L. Bayón, J.A. Fernández-Rubiera. Predicting beam and diffuse horizontal irradiance using Fourier expansions. *Renewable Energy* **154**, 46-57 (2020).